Progress In Electromagnetics Research C, Vol. 32, 109–122, 2012

WIDEBAND MICROWAVE CROSSOVER USING DOUBLE VERTICAL MICROSTRIP-CPW INTERCONNECT

Y. Wang*, A. M. Abbosh, and B. Henin

School of ITEE, The University of Queensland, St. Lucia, QLD 4072, Australia

Abstract—The paper presents the design of a novel ultra-wideband microwave crossover for the use in microstrip circuits. The proposed structure includes a double microstrip-coplanar waveguide (CPW) vertical interconnect in single-layer substrate technology which allows an inclusion of a finite-width coplanar waveguide (CPW) on the top side of the substrate to achieve the required cross-link. The presented design is verified using the full-wave electromagnetic simulator Ansoft HFSS v.13 and experimental tests. The obtained experimental results show that in the frequency band of 3.2–11 GHz, the crossover has an isolation of 20 dB accompanied by insertion losses of no more than 1.5 dB.

1. INTRODUCTION

A microwave crossover is a circuit which allows the crossing of two microwave transmission lines while maintaining a proper isolation between them. Planar crossovers are increasingly needed in monolithic microwave integrated circuits, microwave multichip modules and many other microwave planar sub-systems which require the signal crossing without disturbing the performance of the already existing circuits.

Planar crossovers can be constructed using wire bond or air bridges [1, 2]. In addition, they can be formed using wired vias using additional substrate layers [3–5]. Although wire bonds and air bridges do their role well, they require specialized equipment for their construction. They also need additional circuits to compensate for their parasitic elements. In turn, wired vias require multiple substrate

Received 19 July 2012, Accepted 22 August 2012, Scheduled 5 September 2012

* Corresponding author: Yifan Wang (yfwang@itee.uq.edu.au).

and conductor layers, which lead to increased fabrication complexity. In another approach, a crossover is designed by locating two microstrip feeding lines at one layer and the other two at a different layer [6]. However, such a design is incompatible with microstrip circuits and violates the fundamental of crossover design that requires the four ports to be at the same layer.

In order to overcome the shortcomings of wire bonds, air bridges and wired vias, different configurations of crossovers, such as cascaded couplers, ring and multi-section branch-line couplers, have recently been proposed [7–12]. The main drawback of those structures is their limited bandwidth. This is a critical issue in the modern high capacity communication systems.

In another approach to achieve a wideband performance, the authors of [13] proposed a wideband via-free crossover that uses a via-less microstrip to co-planar waveguide (CPW) transition. In that proposed approach, an earlier work on via-less microstrip to coplanar waveguide transitions described in [14–16] are utilized. That design is demonstrated in the 2–8 GHz band showing isolation of 32 dB and in-band insertion loss and return loss of 1.2 dB and 18 dB respectively over more than 44% of bandwidth with respect to the centre frequency of 5 GHz. In [17], several two-port and four-port microstrip to slotline transitions are utilized to build a crossover with 40% fractional bandwidth.

In this paper, we propose an alternative configuration of wideband microwave via-less crossover. Similarly as in [13], the new structure is accomplished in single-layer substrate technology, in which two conducting coatings of the substrate are used in the design process. The essential part of this crossover is a double vertical interconnect which is established in the microstrip-CPW technique. This interconnect has microstrip ports on top side of the substrate making it compatible with ordinary microstrip circuits. In order to achieve low insertion losses and high isolation between two crossing transmission lines, a CPW of finite width with transitions to microstrip ports on the top layer of the substrate is used.

The crossover is designed with the aid of a full-wave electromagnetic simulator HFSS. The goal is to obtain broadband performance from 3 to 11 GHz, which conforms to the ultra wide frequency band (3.1–10.6 GHz) specified by the Federal Communications Commission (FCC) authority. The design process is explained in Section 2. The simulation and experimental results are presented in Section 3. The concluding remarks are made in Section 4.

2. DESIGN

The configurations of a double vertical interconnect which is proposed for the construction of a new via-less crossover is shown in Figure 1.

This interconnect uses elliptically shaped microstrip patches in the top layer and elliptically shaped slots and patches in the bottom layer of a two-side conductor coated dielectric substrate. The level of electromagnetic coupling between the two sides of the substrate is controlled by adjusting the dimensions D_m, D_c, and D_s. The structure is introduced in [18] to obtain an ultrawideband (3–10 GHz) phase shifter. Its design stemmed from the earlier work on UWB couplers [19, 20] which indicates the possibility of achieving a tight coupling across an ultra-wideband using broadside-coupled structures.

The convenience of the structure of Figure 1 is that in addition to an approximately constant phase shift (compared with a suitable length of reference microstripline) it offers a small insertion loss between ports 1 and 2 across the band of 3–10 GHz. This property is of interest to the current design of crossover. Its other advantageous feature is that it has microstrip ports which make it compatible with ordinary microstrip circuits.

By closely inspecting the structure of Figure 1, it can be noticed that it offers the possibility of including a microstrip line or other types of planar conducting lines in the region between Sections 1 and 2. Such a new transmission line can be run on the top side of the substrate and in the direction perpendicular to the CPW in the bottom layer. However, this requires a further separation of the two conducing elliptical patches on top side of the substrate to minimize the coupling between the two links. Therefore, it is necessary to investigate how this increased separation affects the electrical performance of the

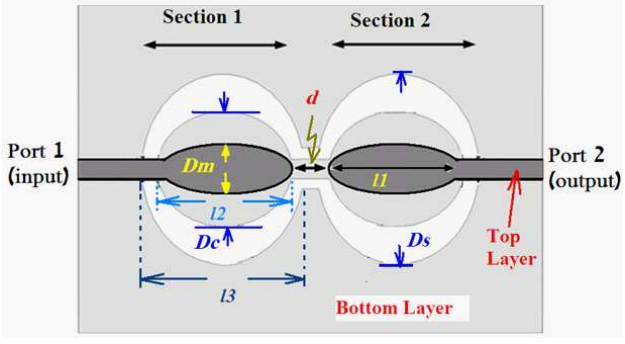

Figure 1. Configuration of double vertical interconnect [18].

Table 1. Values of the design parameters for the interconnect.

Parameter	Value (mm)
Dm	2.24
Dc	1.68
Ds	4.48
l_1	2.8
l_2	2.8
l_3	3.2

double vertical interconnect of Figure 1. Here, the investigations are performed assuming Rogers RT6010 with thickness 0.635 mm, dielectric constant 10.2 and tangent loss 0.0023 as the substrate.

The dimensions of the utilized interconnect are calculated using the conformal mapping method as explained in [18]. For an ultra-wideband performance, the microstrip patch at the top layer and the CPW patch at the bottom layer are designed to be tightly coupled. In the current design the coupling factor C between the top microstrip layer and the bottom CPW layer is taken as 0.8. Using the method in [18], the initial values of the widths (D_m, D_c, D_s) can be calculated. The initial lengths of the microstrip and CPW patches (l_1, l_2 and l_3) are chosen to be around quarter wavelength at the centre of the required band. The final dimensions are then optimized for a maximum possible bandwidth with more than 10 dB return loss at the two ports of interconnect are obtained using the optimization feature of the simulation tool HFSS. The dimensions listed in Table 1 are found.

The remaining design parameter of the structure depicted in Figure 1 is the length of the CPW (d) connecting the two microstrip/CPW transitions forming the interconnect. In the design of a phase shifter [18], d is chosen to be as small as possible for a compact structure. However, in the current work which involves using the same structure to build a crossover, d cannot be very small due to the need to minimize the coupling between the two pairs of ports forming the crossover as will be explained later. Thus, the effect of the length d is to be included in the design of the interconnect.

It is possible to extend the analysis presented in [18] to include the effect of the design parameter d. It represents a CPW transmission line that is assumed to be lossless and perfectly matched with the two coupled CPW patches. Hence, it only introduces a phase shift equals to $e^{-j\beta d}$ on the signal passing through it. β is the phase constant of the CPW line, Following the analysis of the multi-section coupled

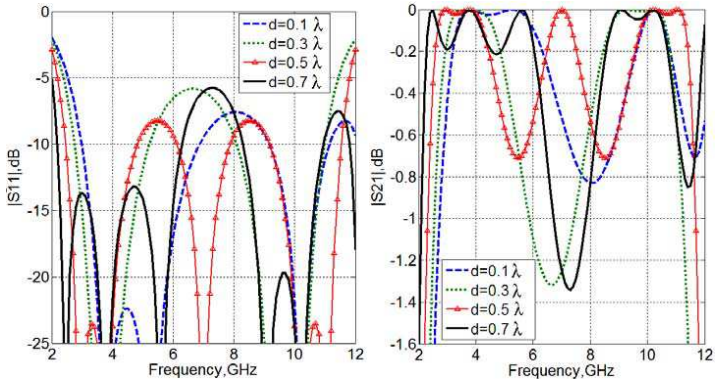

Figure 2. Analytical calculation of the S parameters (S_{11} and S_{21}) for different values of d.

structures [15], it is possible to show that the effective reflection coefficient (S_{11}) and transmission coefficient (S_{21}) for the structure of Figure 1 are given as

$$S_{11} = \alpha + \frac{\delta^2 \alpha e^{-j2\beta d}}{1 - \alpha^2 e^{-j2\beta d}}; \quad S_{21} = \frac{\delta^2 e^{-j\beta d}}{1 - \alpha^2 e^{-j2\beta d}} \tag{1}$$

$$\alpha = \frac{1 - C^2\left(1 + \sin^2(\beta l_1)\right)}{\left[\sqrt{1 - C^2}\cos(\beta l_1) + j\sin(\beta l_1)\right]^2} \tag{2}$$

$$\delta = \frac{j2C\sqrt{1 - C^2}\sin(\beta l_1)}{\left[\sqrt{1 - C^2}\cos(\beta l_1) + j\sin(\beta l_1)\right]^2} \tag{3}$$

where l_1 is the physical length of the coupled structure.

The derived model (1)–(3) is used to investigate the effect of the parameter d on the performance. In the calculations, it is assumed that $C = 0.8$, and $l_1 = \lambda/4$, λ is the effective wavelength at the centre of the band ($f_0 = 7\,\text{GHz}$). The variation of the S parameters (S_{11}, S_{21}) for the interconnect shown in Figure 1 at different values of d is depicted in Figure 2. It is clearly seen that, for a minimum insertion loss across a widest bandwidth, d should be around 0.5λ.

In order to verify the theoretical model, a full-wave electromagnetic simulator is used to calculate the performance for different values of d. Figure 3 shows the full-wave electromagnetic simulations results for the return loss (Figure 3(a)) and insertion loss (Figure 3(b)) of the double interconnect of Figure 1 when d is varied. The obtained results show that increasing the separation between the two sections

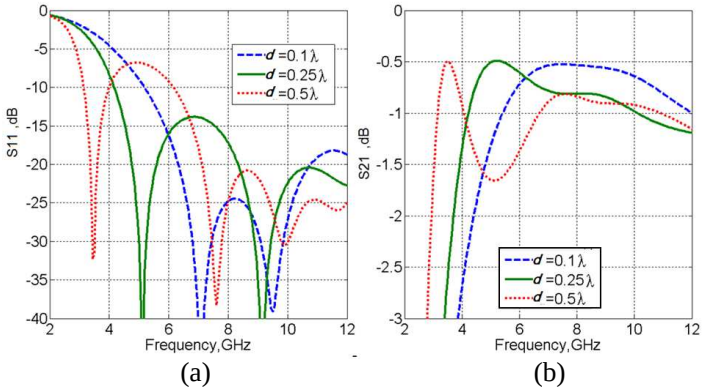

Figure 3. Simulated results for (a) S_{11} and (b) S_{12} of the double interconnect for different values of d.

of the structure of Figure 1 increases the bandwidth of the structure as predicted in theory. The full-wave simulations agree with the theory in showing that the optimum choice for the length of the CPW (d) should be around 0.5λ. Increasing d beyond that value is not a preferred option for two reasons. Firstly, the structure is required to be compact. Thus, the lowest possible value for d that achieves the required bandwidth should be used. Secondly, increasing the length of CPW (d) significantly increases the possibility of radiation losses from the structure especially at the upper part of the band. These kinds of losses are also observed in [10]. They can be minimized using a suitable enclosure.

After choosing a suitable separation between the two sections of the structure of Figure 1 depending on the acceptable level of insertion loss, the required bandwidth and the needed space for the additional crossing line, the next step is to include the crossing transmission line. The natural choice is to use a microstrip line as it directly offers two new microstrip ports 3 and 4. However, this needs to be investigated to find whether an inclusion of such a transmission line can provide low insertion losses and good isolation between the pairs of ports 1, 2 from 3, 4. The configuration of cross-over formed by the interconnect of Figure 1 and the $50\,\Omega$ microstrip line, accompanied by the simulated results for return loss, isolation and transmission coefficients is presented in Figure 4. For $50\,\Omega$ characteristic impedance, the microstrip line is designed to have a width of 0.56 mm. The length of CPW is $d = 9$ mm, which is around 0.5λ as predicted in the theory.

The results presented in Figure 4 indicate that the crossover employing a microstrip line as the second transmission line produces

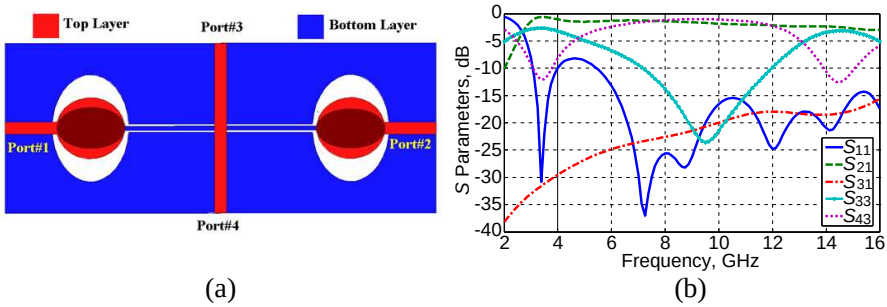

Figure 4. (a) Simulated structure of the crossover incorporating the double interconnect and the microstripline. (b) Simulation results for its scattering matrix parameters.

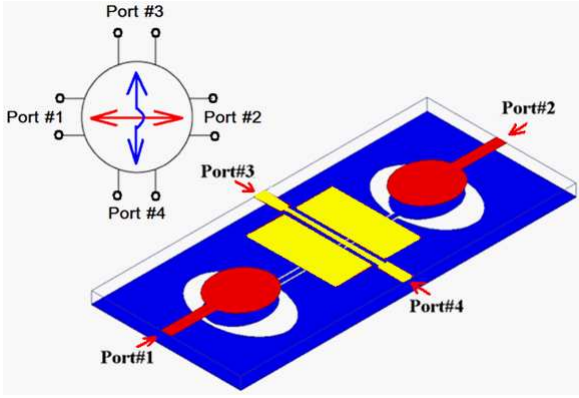

Figure 5. Structure of the new crossover incorporating the double interconnect and finite width CPW crossing line.

a good performance within the frequency band from 7 to 12 GHz with insertion losses smaller than 1.5 dB and isolation more than 17 dB. The reason for not maintaining good return (S_{33}) and insertion losses (S_{21}, S_{43}) outside the 7–12 GHz band is that the fields carried by the microstrip line at the top layer couple to those of the CPW at the bottom layer and thus perturb each other.

In general, an improved insertion loss and isolation between the two transmission lines can be achieved using a two-fold strategy. One is an increased spatial separation of fields carried by CPW in the ground and a new transmission line on top of substrate and the other is the use of cross-polarized fields carried by the two lines. This strategy is investigated next.

One possibility of getting spatially separated cross-polarized electric fields is to split the section of microstrip line over-passing the CPW of Figure 3(a) into three parts to force the vertical electric field from the region below the microstrip to the horizontal plane in the three strip region. This idea is tried and proven to introduce only a slight improvement in performance of the crossover. A more viable alternative is to use a three-conductor line but in the form of CPW. This alternative, in which the finite width CPW is used instead of microstrip line, is presented in Figure 5. The crossover layout also includes CPW to microstrip transitions so that all the four ports are of microstrip type.

3. EQUIVALENT CIRCUIT MODEL

To fully understand the operation of the proposed crossover, the equivalent circuit model of the device is depicted in Figure 6. The microstrip to CPW transition can be represented as a transformer with a certain turns ratio (n_1) [21]. The value of n_1 depends on the level of coupling between the two transmission lines. For a properly designed transition, the ratio n is close to 1. Similarly, the uniplanar microstrip to CPW transitions can be represented by a transformer with another turns ratio (n_2) that can also be close to 1 for a properly designed transition. The normal-angle intersection of the CPW at the top layer and the CPW at the bottom layer at a very small area guarantees a very low level coupling between them. In the equivalent circuit depicted in Figure 6, this is equivalent to having a transformer with a very low turns ratio (n_3) connecting the circuits of the two crossing lines.

The open-ended elliptical microstrip patches at the top layer and the elliptical CPW patches at the bottom layer have lengths equal to quarter of the effective wavelength at the centre of the band. Thus, they are represented as quarter wavelength transmission lines (θ_m and

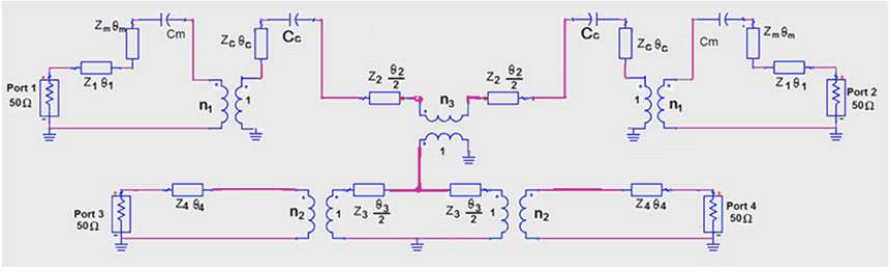

Figure 6. Equivalent circuit model of the proposed crossover.

θ_c) in the equivalent circuit. The low value capacitors C_m and C_c are included in the circuit to represent the fringe effects at the open-ended microstrip and CPW at the two transitions. As derived in the theory, the length of the CPW line at the bottom layer (θ_2) is chosen to be around half a wavelength. The length of the CPW line at the top layer (θ_3) is chosen similarly. The lengths of the feeders at the four ports (θ_1 and θ_4) are not critical parameters in the design and can be chosen as short as possible for a compact structure. The impedances of all the lines shown in Figure 6 are designed to be 50 Ω.

By inspecting the equivalent circuit of Figure 6, it is possible to predict that the signal input at port #1 emerges from port #2. Only a small part of that signal leaks to the ports #3 and 4 due to the very small value of the turns ratio n_3. Similarly, if a signal is applied to port #3, most of that signal emerges from port #4 with only a very small part leaking to the ports #1 and 2. Since all the transmission lines used to build the crossover are designed to have 50 Ω impedance, a good matching is expected at all the four ports. Those conclusions from the equivalent circuit are the required performance for the designed crossover. For the practical circuit, the validity of those conclusions depends on the careful design of the four transitions used to build the device.

4. RESULTS

Following the above considerations, the design of a new crossover shown in Figure 5 for operation in the frequency band from 3.1 to 10.6 GHz is attempted. The design is carried out with the aid of full-wave EM software. Rogers RT6010 with thickness 0.635 mm, dielectric constant 10.2 and tangent loss 0.0023 is assumed as the substrate.

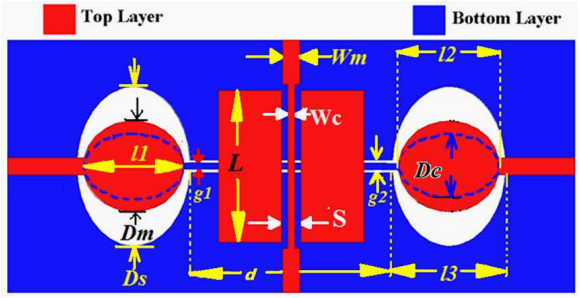

Figure 7. Layout of the planar crossover structure including design parameters.

Table 2. Values of the design parameters for the crossover.

Parameter	Description	Value (mm)
Dm	Short radius of microstrip short-circuit elliptical stub	2.24
Dc	Short radius of ground short-circuit elliptical stub	1.68
Ds	Short radius of ground slot open-circuit elliptical stub	4.48
l_1	Long radius of microstrip short-circuit elliptical stub	2.8
l_2	Long radius of ground short-circuit elliptical stub	2.8
l_3	Long radius of ground slot open-circuit elliptical stub	3.2
L_{CPW}	Length of bottom layer CPW line	8
Wm	Width of feeding microstrip line	0.56
Wc	Width of crossing CPW central line	0.3
S	Width of crossing CPW side slot	0.7
g_1	Width of bottom layer CPW central line	0.3
g_2	Width of bottom layer CPW side slot	0.7
L	Length of crossing finite CPW line	6

Figure 7 shows layout of the crossover structure including its design parameters. Table 2 presents parameters of the crossover as obtained from initial design procedure explained earlier followed by a further tuning with full-wave EM analysis and design software. As can be gathered from Table 2, the designed crossover features quite a small size, which is welcome in many applications offering only a small space for its implementation.

Using the above parameters, the crossover is manufactured and its photograph is shown in Figure 8. It is augmented with SMA connectors to carry out the experimental tests. The experimental

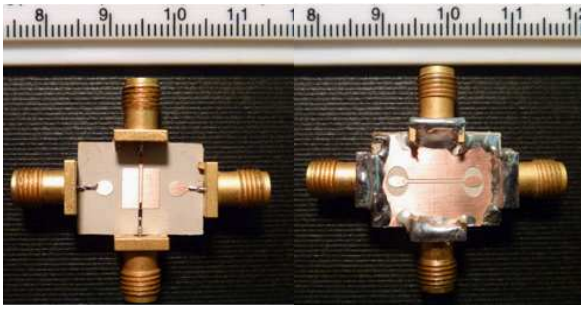

(a) (b)

Figure 8. Photograph of the manufactured crossover, (a) top and (b) bottom view.

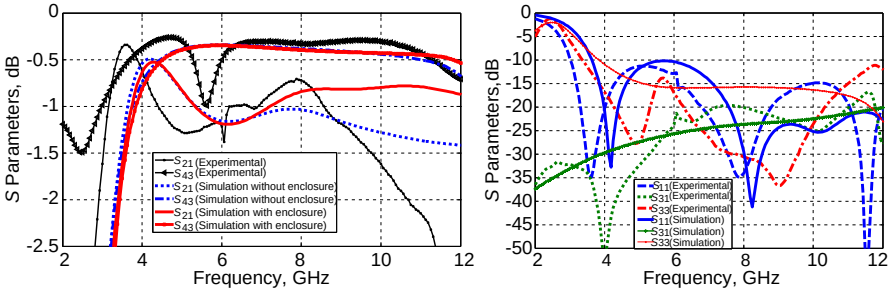

(a) (b)

Figure 9. Simulated and measured (a) insertion loss and (b) return loss and isolation of the crossover.

tests also consider the effects of the residual radiation and the use of shielding for minimizing it.

Figure 9 shows the simulated and measured results for magnitudes of the scattering matrix parameters of the designed crossover over the frequency band from 2 to 12 GHz. From the obtained results, it is observed that both the simulated and measured insertion loss between ports 1 and 2 varies between 0.7 and 1.3 dB in the frequency band of 3.2–11 GHz. In turn, the simulated and measured return loss of port 1 is greater than 10 dB in the frequency band from 3.2 to 12 GHz. The simulated and measured insertion loss between ports 3 and 4 varies between 0.4 and 1 dB in the frequency band from 3.2 to more than 11 GHz. The simulated and measured return loss of port 3 is greater than 10 dB in the frequency band of 3.2–12 GHz. The simulated and measured isolation between port 1 and port 3 is more than 18 dB for

the whole investigated frequency range from 3 to 12 GHz.

It is believed that the insertion losses in the passband of the developed device are caused by several factors, such as the dielectric and conductor losses of the utilized substrate, the sub-miniature A (SMA) connectors and radiation from the different parts of the crossover. While, we do not have control over the substrates and SMA losses, we investigated the level of radiation loses by enclosing the crossover in a metallic box. To that end, the performance of the designed crossover with the enclosure is simulated. The result of simulation is shown in Figure 9(a). It is found that the printed structure inserted into a metallic box of dimensions 14 mm × 20 mm × 10 mm helps in preventing any radiation from the structure, especially at the upper part of the band where a slight improvement in the performance is observed.

5. CONCLUSIONS

In this paper, the design of a novel microwave crossover for the use in microstrip circuits has been presented. The proposed structure includes a double vertical interconnect in single-layer substrate and microstrip-CPW technology which allows an inclusion of a finite-width CPW on top of the substrate to achieve the signal cross link. The proposed circuit utilizes two sides of the substrate in the way it is compatible with ordinary microwave microstrip circuits. The presented design has been verified using full-wave electromagnetic field analysis and experimental tests. The proposed crossover has an ultrawideband performance with less than 1.5 dB insertion loss and more than 20 dB isolation across the band from 3.2 GHz to 11 GHz using a compact structure.

ACKNOWLEDGMENT

The authors acknowledge the financial support of the Australian Research Council in the form of Discovery Project Grant DP0986429. We also acknowledge Mr. J. Kohlbach of the Electronic Workshop, The University of Queensland for manufacturing the device, and Prof. M. Bialkowski for initiating the investigation.

REFERENCES

1. Chiu, J.-C., J.-M. Lin, M.-P. Houng, and Y.-H. Wang, "A PCB compatible 3-dB coupler using microstrip-to-CPW via-hole

transitions," *IEEE Microwave and Wireless Components Letters*, Vol. 16, No. 6, 369–371, Jun. 2006.

2. Horng, T., "A rigorous study of microstrip crossovers and their possible improvements," *IEEE Trans. Microw. Theory Tech.*, Vol. 42, No. 9, 1802–1806, Sep. 1994.
3. Martoglio, L., E. Richalot, G. Lissorgues, and O. Picon, "A wideband 3D-transition between coplanar and inverted microstrip on silicon to characterize a line in MEMS technology," *Microwave and Optical Tech. Lett.*, Vol. 46, No. 4, 378–381, 2005.
4. Burke, J. and R. Jackson, "Surface-to-surface transition via electromagnetic coupling of microstrip and coplanar waveguide," *IEEE Trans. Microw. Theory Tech.*, Vol. 37, No. 3, 519–525, Mar. 1989.
5. Liu, W., Z. Zhang, Z. Feng, and M. F. Iskander, "A Compact wideband microstrip crossover," *IEEE Microwave and Wireless Components Letters*, Vol. 22, No. 5, 254–256, May 2012.
6. Kusiek, A., W. Marynowski, and J. Mazur, "Design of a broadband microstrip crossover for ultra-wideband applications," *Microw. Opt. Technol. Lett.*, Vol. 52, No. 5, 1100–1104, 2010.
7. Chiou, Y., J. Kuo, and H. Lee, "Design of compact symmetric four-port crossover junction," *IEEE Microwave and Wireless Components Letters*, Vol. 19, 545–447, 2009.
8. Yao, J., C. Lee, and S. Yeo, "Microstrip branch-line couplers for crossover application," *IEEE Trans. Microw. Theory Tech.*, Vol. 59, 87–92, 2011.
9. Wong, F. and K. Cheng, "A novel, planar, and compact crossover design for dual-band applications," *IEEE Trans. Microw. Theory Tech.*, Vol. 59, 568–573, 2011.
10. De Ronde, F. C., "Octave-wide matched symmetrical, reciprocal, 4- and 5 ports," *1982 IEEE MTT-S International Microwave Symposium Digest*, 521–523, Jun. 15–17, 1982.
11. Chen, Y. and S. Yeo, "A symmetrical four-port microstrip coupler for crossover application," *IEEE Trans. Microw. Theory Tech.*, Vol. 55, No. 11, 2434–2438, 2007.
12. Abbosh, A., "Planar wideband crossover with distortionless response using dual-mode microstrip patch," *Microw. Opt. Technol. Lett.*, Vol. 54, No. 9, 2077–2079, 2012.
13. U-yen, K., E. J. Wollack, S. H. Moseley, T. R. Stevenson, W.-T. Hsieh, and N. T. Cao, "Via-less microwave crossover using microstrip-CPW transitions in slotline propagation mode I," *2009 IEEE MTT-S International Microwave Symposium Digest*, 1029–

1032, 2009.

14. Lin, T.-H., "Via-free broadband microstrip to CPW transition," *Electronics Letters*, Vol. 37, No. 15, 960–961, Jul. 19, 2001.
15. Girard, T., R. Staraj, E. Cambiaggio, and F. Muller, "Microstrip-CPW transitions for antenna array applications," *Microw. Opt. Technol. Lett.*, Vol. 23, No. 3, 131–133, 1999.
16. Jin, H., R. Vahldieck, J. Huang, and P. Russer, "Rigorous analysis of mixed transmission line interconnects using the frequency-domain TLM method," *IEEE Trans. Microw. Theory Tech.*, Vol. 41, 2248–2255, 1993.
17. Abbosh, A., "Wideband planar crossover using two-port and four-port microstrip to slotline transitions," *IEEE Microwave and Wireless Components Letters*, Vol. 22, No. 9, 2012.
18. Abbosh, A. M., "Broadband fixed phase shifters," *IEEE Microwave and Wireless Components Letters*, Vol. 21, No. 1, 22–24, 2011.
19. Abbosh, A. M. and M. E. Bialkowski, "Design of compact directional couplers for UWB applications," *IEEE Trans. Microw. Theory Tech.*, Vol. 55, No. 2, 189–194, Feb. 2007.
20. Abbosh, A. M. and M. E. Bialkowski, "Design of ultra wideband 3DB quadrature microstrip/slot coupler," *Microw. Opt. Technol. Lett.*, Vol. 49, No. 9, 2101–2103, 2007.
21. Gupta, K. C., R. Garg, I. Bahl, and P. Bhartia, *Microstrip Lines and Slotlines,* Artech House, 1996.